

Visualizing charge transport in silicon nanocrystals embedded in SiO₂ films with electrostatic force microscopy

Lau, Hon Wu; Ng, Chi Yung; Liu, Yang; Tse, Man Siu; Lim, Vanissa Sei Wei; Tan, Ooi Kiang; Chen, Tupei

2004

Lau, H. W., Ng, C. Y., Liu, Y., Tse, M. S., Lim, V. S. W., Tan, O. K., et al. (2004). Visualizing charge transport in silicon nanocrystals embedded in SiO₂ films with electrostatic force microscopy. *Applied physics letters*, 85(14), 2941-2943.

<https://hdl.handle.net/10356/101362>

<https://doi.org/10.1063/1.1801675>

Applied Physics Letters © copyright 2004 American Institute of Physics. The journal's website is located at http://apl.aip.org/applab/v85/i14/p2941_s1?isAuthorized=no

Downloaded on 23 Aug 2022 04:35:00 SGT

Visualizing charge transport in silicon nanocrystals embedded in SiO₂ films with electrostatic force microscopy

C. Y. Ng, T. P. Chen,^{a)} H. W. Lau, Y. Liu, M. S. Tse, and O. K. Tan

School of Electrical and Electronic Engineering, Nanyang Technological University, Singapore 639798, Singapore

V. S. W. Lim

Institute of Microelectronics, 11 Science Park Road, Singapore 117685, Singapore

(Received 27 April 2004; accepted 3 August 2004)

In this work, we report a mapping of charge transport in silicon nanocrystals (nc-Si) embedded in SiO₂ dielectric films with electrostatic force microscopy. The charge diffusion from charged nc-Si to neighboring uncharged nc-Si in the SiO₂ matrix is found to be the dominant mechanism for the decay of the trapped charge in the nc-Si. The trapped charge and the charge decay have been determined quantitatively from the electrical force measurement. An increase in the area of the charge cloud due to the charge diffusion has been observed clearly. In addition, the blockage and acceleration of charge diffusion by the neighboring charges with the same and opposite charge signs (i.e., positive or negative), respectively, have been observed. © 2004 American Institute of Physics. [DOI: 10.1063/1.1801675]

Research on silicon dioxide embedded with silicon nanocrystals (nc-Si) has been carried out intensively over the past decade due to the potential applications of nc-Si in memory devices as well as optoelectronic devices.^{1–3} To enable SiO₂ with embedded nc-Si to work as a nonvolatile memory device, understanding the charge transport in the material system is indeed important. By using the conductive atomic force microscope method,⁴ localized charging effect in nc-Si has been shown to exhibit good charge retention. On the other hand, the charging of Co nanoclusters and silver nanocrystals has been characterized recently with electrostatic force microscopy (EFM).^{5,6} With the EFM technique, information of electrical properties can be obtained with nanometer resolution and the distribution of charges trapped in the nanocrystals embedded in the thin film can be mapped based on the total electrostatic potential of the cantilever tip.^{7,8} This is very useful to the study of the charge dissipation of nc-Si embedded in SiO₂ dielectric films. In this letter, it is shown that the dominant charge decay mechanism during discharging of nc-Si is the diffusion of charges from a charged nc-Si to the surrounding uncharged nc-Si. This phenomenon has been clearly observed with noncontact EFM mode in this study.

SiO₂ films were thermally grown to 750 nm on N-type (100) oriented Si wafers in dry oxygen at 950°C. The silicon wafers were phosphorous-doped with a concentration of $2 \times 10^{15} \text{ cm}^{-3}$. Si⁺ ions with a dose of $3 \times 10^{16} \text{ cm}^{-2}$ were then implanted to the SiO₂ thin films at 10 keV. The peak concentration was found at a depth of about 10 nm as obtained from the secondary ion-mass spectroscopy measurement. Thermal annealing was carried out at 1000°C in N₂ ambient for 1 h to induce nc-Si formation. The back sides of wafers were coated with a layer of aluminum with the thickness of about 1 μm after removing the back side oxide. Finally, metal alloy process was conducted at 425°C in N₂ ambient to form ohmic contacts. For comparison, one quarter of each of the wafers was not implanted with Si⁺ ions (i.e., only pure

SiO₂ thin films on Si substrate). EFM studies were performed at room temperature under ambient conditions in air with a Veeco/Digital Instrument Dimension 3000 Scanning Probe Microscope.

To visualize charging effect of nc-Si embedded in SiO₂, the total force acting on the EFM tip due to the Coulomb interaction between the sample surface and the tip is measured with the EFM.⁹ During the EFM imaging, the tip is scanned over the sample surface with a constant height. From the two-dimensional (2D) image of EFM, the quantity of stored charge in nc-Si can be estimated based on the force arising from the Coulomb interactions between the charge of the sample and the charge on the tip. For the samples used in this study, nc-Si distributed from the surface to a depth of ~20 nm with the peak concentration at a depth of ~10 nm. The nc-Si distribution can be represented with a nc-Si surface layer in the SiO₂ film, and the surface layer thickness is ~20 nm, which is much smaller than the SiO₂ film thickness (750 nm). Therefore, based on the formula of force given in Refs. 5 and 8, the total electrostatic force on the tip can be written as

$$F(z) = \frac{1}{\left(z + \frac{d}{\epsilon}\right)^2} \left(\frac{-\epsilon_0 A V^2}{2} + \frac{d Q V}{\epsilon} - \frac{d^2 Q^2}{2 \epsilon^2 \epsilon_0 A} \right), \quad (1)$$

where z is the distance between the tip and the sample, d is the SiO₂ film thickness, ϵ is dielectric constant of SiO₂, Q is the charges trapped in the nc-Si, A is the area of the charged region, and V is the EFM dc bias. The measurement of force is based on the shift in the tip cantilever resonance frequency with respect to its nominal frequency.

This shift is related to the Coulomb force gradient detected by the EFM tip and can be written as¹⁰

$$\frac{2k\Delta f}{f_0} = \frac{\partial F(z)}{\partial z}, \quad (2)$$

where Δf is the shift of resonance frequency, f_0 is the nominal frequency, and k is the cantilever spring constant esti-

^{a)}Electronic mail: echentp@ntu.edu.sg

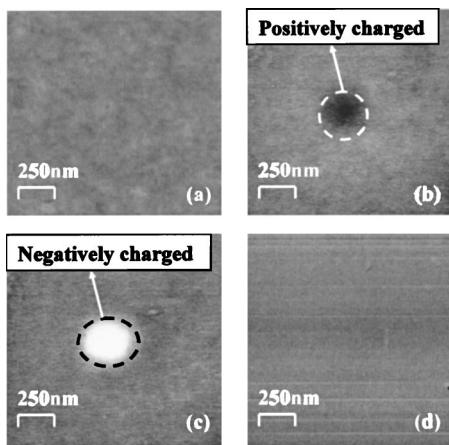


FIG. 1. EFM images. (a) Uncharged nc-Si sample; (b) nc-Si sample charged at +4 V; (c) nc-Si sample charged at -4 V; and (d) SiO₂ sample (i.e., without nc-Si) charged at +4 V.

mated from the lever geometry. The total charge Q is then estimated with the above equations.

Figure 1 shows the comparison of 2D EFM images of SiO₂ films with and without nc-Si before (i.e., virgin) and after charge injection. The charge injection is carried out by making the EFM tip contact the sample surface and applying a bias to the tip. A low bias of +4 or -4 V is applied on either the virgin nc-Si sample or the control pure SiO₂ sample for 10 s. Charge trapping in the dielectric films is evident from the bright or dark spots in the EFM images. The EFM images are obtained by applying a bias of -1 V to the EFM tip and with the noncontact scanning mode. With the bias of -1 V, a bright spot indicates negative charge trapping while a dark spot indicates positive charge trapping. For the virgin nc-Si sample and the control sample (i.e., pure SiO₂ without nc-Si), there are no spots observed, indicating no charge trapping [Fig. 1(a) and 1(d)]; however, for the nc-Si samples after the +4 and -4 V bias, dark and bright spots appear, showing positive and negative charge trapping, respectively [Figs. 1(b) and 1(c)]. As can be seen in Fig. 1, for the tip radius of 15 nm, the size of the charged area detected is ~250 nm.

To understand the charge transport in nc-Si, charge decay from the dielectric film is monitored with a series of snapshots of EFM images recorded in real time after constant voltage injection. The contrast of the bright or dark spots

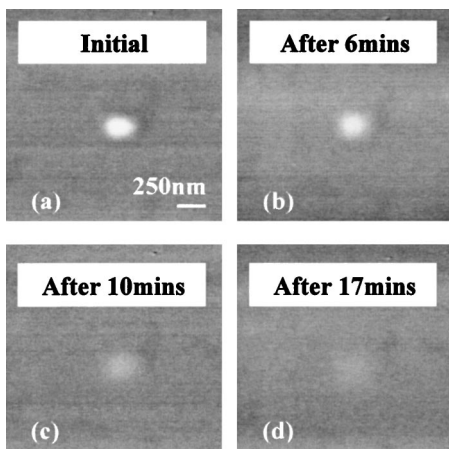


FIG. 2. EFM images of decay of charge trapped in nc-Si.

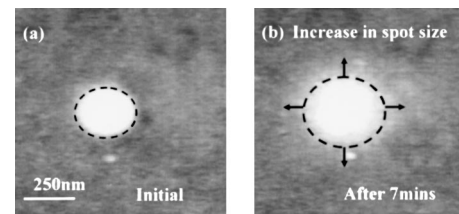


FIG. 3. Increase of the area of the charge cloud due to charge diffusion.

observed in the EFM image diffuses over time, as shown in Fig. 2, indicating dissipation of the injected charge. After a long time, the contrast disappears indicating that the trapped charge decays to the background level. The dissipation of the trapped charges is actually due to the diffusion of the trapped charges to the neighboring uncharged nc-Si in the surrounding area. The charge diffusion leads to the increase in the area of the charge cloud (i.e., the area of the charged spot) together with the reduction in the brightness (or darkness) of the charged spot. One typical example is shown in Fig. 3. The increase of the area of the bright spot (electron trapping) can be clearly seen in this figure.

To study the influence of neighboring charges on the charge decay, we have created one charged spot, two charged spots with a spacing of 300 nm, and three charged spots on a straight line with a spacing of 300 nm. For the cases of two

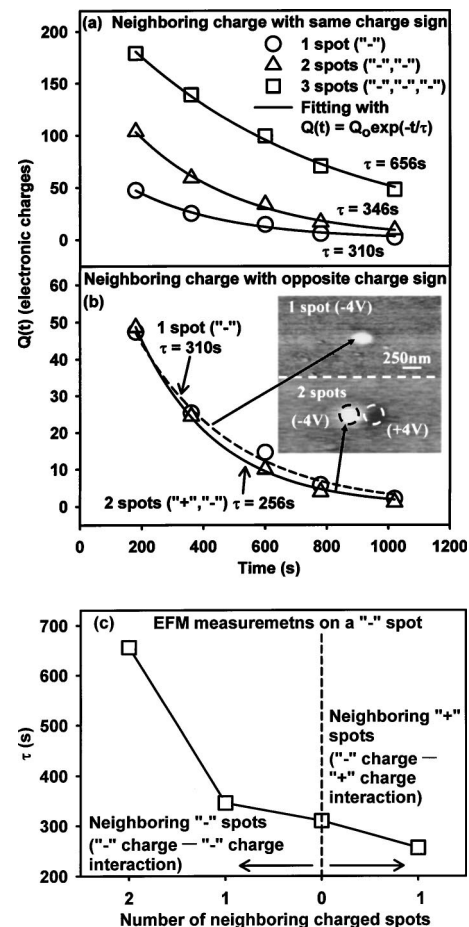


FIG. 4. (a) Blockage of charge diffusion by neighboring charges with the same charge sign; (b) acceleration of charge diffusion by neighboring charges with the opposite sign; and (c) decay time as a function of both the number and charge sign of the neighboring charged spots. "+" represents positive charge while "-" represents negative charge.

charged spots, the charge in one spot has the sign (positive or negative) either the same as or opposite to that of another spot. For the cases of one and three charged spots, each spot is negatively charged. Such an arrangement can give us a clear picture of the influence of neighboring charges on the charge diffusion. To have quantitative information of charge decay, we have determined the charge Q with Eq. (1), and the charge decay with time is shown in Fig. 4.

First, we study the influence of the neighboring charges with the same charge sign by applying -4 V bias for 10 s for each spot to create one to three charged spots, and the results are shown in Fig. 4(a). Note that for the negative bias each spot is negatively charged. As shown in Fig. 4(a), the charge decay for the all cases is found to follow the exponential law, i.e., $Q(t) = Q_0 \exp(-t/\tau)$, where Q_0 is the initial charge, t is the time after charge injection, and τ is the characteristic decay time. The characteristic decay time is 310, 346 and 656 s for one, two, and three charged spots, respectively. The increase in the characteristic decay time with the spot number clearly shows the blockage of charge diffusion by the neighboring charges with the same sign. In contrast, the neighboring charge with opposite sign (i.e., one spot is negatively charged and the other spot is positively charged) can speed up the charge decay, as shown in Fig. 4(b). To show a clear picture of the effect of charge-charge interaction, the decay time as a function of both the number and charge sign of the neighboring charged spots is shown in Fig. 4(c). Note that the EFM measurement is conducted on a negatively charged spot. As shown in Fig. 4(c), the neighboring negative charge blocks the charge diffusion of the negatively charged spot under measurement, leading to a longer decay time; however, the neighboring positive charge promotes the dissipation of the negatively charge spot under measurement, leading to a shorter decay time.

In conclusion, charge transport in nc-Si embedded in SiO₂ dielectric films can be visualized with EFM. The charge diffusion from charged nc-Si to the surrounding neighboring uncharged nc-Si in the SiO₂ matrix is found to be the dominant mechanism for the decay of the trapped charge in the nc-Si. The trapped charge in nc-Si and the charge decay have been determined quantitatively from the electrical force measurement. An increase in the area of the charge cloud due to the charge diffusion has been observed clearly. In addition, the blockage and acceleration of charge diffusion by the neighboring charges with the same and opposite charge signs, respectively, have been observed also.

This work has been financially supported by The Ministry of Education of Singapore under Project No. ARC 1/04. The author would like to thank Dr. Alastair Trigg from Institute of Microelectronics for the equipment support.

¹C. Garcia, B. Garrido, P. Pellegrino, R. Ferre, J. A. Moreno, J. R. Morante, L. Pavesi, and M. Cazzanelli, *Appl. Phys. Lett.* **82**, 1595 (2003).

²S. Tiwari, F. Rana, H. Hanafi, A. Hartstein, E. F. Crabbe, and K. Chan, *Appl. Phys. Lett.* **68**, 1377 (1996).

³Y. Shi, K. Saito, H. Ishikuro, and T. Hiramoto, *J. Appl. Phys.* **84**, 2358 (1998).

⁴E. A. Boer, M. L. Brongersma, H. A. Atwater, R. C. Flagan, and L. D. Bell, *Appl. Phys. Lett.* **79**, 791 (2001).

⁵D. M. Schaadt, E. T. Yu, S. Sankar, and A. E. Berkowitz, *Appl. Phys. Lett.* **74**, 472 (1999).

⁶R. M. Nyffenegger, R. M. Penner, and P. Schierle, *Appl. Phys. Lett.* **71**, 1878 (1997).

⁷G. H. Buh, H. J. Chung, and Y. Kuk, *Appl. Phys. Lett.* **79**, 2010 (2001).

⁸C. Guillemot, P. Budau, J. Chevrier, F. Marchi, F. Comm, C. Alandi, F. Bertin, N. Buffet, Ch. Wyon, and P. Mur, *Europhys. Lett.* **59**, 556 (2002).

⁹Y. Martin, D. W. Abraham, and H. K. Wickramasinghe, *Appl. Phys. Lett.* **52**, 1103 (1988).

¹⁰P. Girard, *Nanotechnology* **12**, 485 (2001).